NOx EMISSION ON RECIPROCAL FILTRATION COMBUSTION OF BIOGAS: A CASE STUDY

W. M. Barcellos,
W. C. Araújo,
G. F. Alves
J. V. T. Alves
L. A. Freire Filho

Universidade Federal do Ceará
Departamento de Engenharia Mecânica
Fortaleza, Ceará, Brazil
william_barcellos@ufc.br

Received: July 15, 2022
Revised: July 19, 2022
Accepted: July 27, 2022

ABSTRACT

Filtration combustion is an effective technique for dealing with low-calorific value fuels, such as derivative fuels from biomass, and simultaneously reducing pollutant emissions. In this study, combustion of biogas (22% of CO2) was investigated theoretically and experimentally by utilizing a reciprocal flow porous burner with heat exchangers inserted in the porous medium. Combustion of lean biogas-air mixtures is stabilized in a naturally transient process, in which a lean equivalence ratio range ($0.1 \leq \Phi \leq 0.9$) and gas flow velocities of 0.2 and 0.3 m/s were employed, periodically switching gas flow direction. Reciprocal flow combustion has been compared with unidirectional combustion, using technical methane as reference gas. In this context, predicted temperature profiles inside the burner, as well as experimental results, have shown that the reciprocating system plays an important role in the combustion process, significantly improving flammability limits, efficiency, and emissions. As result, trapezoidal temperature distribution profiles have been obtained with peaks between 1200 and 1600 K, reaching high efficiency up to 90% and ultra-low emission of nitrogen oxides (≤ 2ppm).

Keywords: Biogas; Filtration Combustion; Reciprocal Flow; Low NOx Emissions

NOMENCLATURE

c_p	fluid specific heat at constant pressure, J/(kg.K)
FC	Filtration Combustion
hc	half cycle, s
v	velocity, m/s
m	mass flow, kg/s
L	length, m
D	diameter, m
y	mass fraction
k	thermal conductivity
x	position. m
T	temperature

Greek symbols

Φ	equivalence ratio
η	efficiency
β	heat loss coefficient, W/K.m³

Subscripts

b	burner
ext	extraction
g	gas flow
inf	inferior
pel	pellets
up	upper
w	water
v	vapor
s	solid phase
f	fluid phase
0	ambient

INTRODUCTION

Biogas is considered to be a promising renewable fuel concerning the emission mitigation of nitrogen oxides (NOx). Unlike natural gas, biogas has a highly variable chemical composition, which directly impacts its combustion characteristics (Kan *et al*., 2018). Biogas composition varies mainly due to the biomass type used in the anaerobic digestion process. This fuel is composed of methane (CH_4) and carbon dioxide (CO_2), along with traces of other gases. Despite the high massic demand of air from methane combustion, the presence of carbon dioxide (CO_2) in the chemical composition of biogas (Matynia *et al*., 2009; Kim *et al*., 2016; Wei *et al*., 2020) (which also diminishes its adiabatic flame temperature) justifies lower NOx indices in practice.

CO_2 does, however, cause some disturbances, such as the decrease in burning velocity, affecting the reaction kinetics and, hence, its propagation, energy conversion efficiency, and even the flame quenching (Xiang *et al*., 2019; Hu *et al*., 2020). Most premixed burners are, however, complex, tightly controlled, and expensive, especially for small- to mid-sized industrial applications, and have difficulty obtaining low NOx emission without sacrificing either CO emissions or system efficiency (Liu *et al*., 2020; Maznoy *et al*., 2021).

The global trend of overall emissions reduction leads to continuous technological advancements. In the energy sector, gas turbines may present NOx emissions below 25 ppm (Karim *et al*., 2017), and some boilers can even produce less than 15 ppm

(Hinrichs *et al*., 2021). Some local regulations, however, may require post-treatment to be fulfilled. The most popular alternative for this case is Selective Catalytic Reduction (SCR), which can reduce up to 90% of the NOx concentration (Cheng and Bi, 2014). Relying on SCR technology, commercial systems with emissions as low as 2.5 ppm are expected.

By taking a comprehensive view on this issue, it is clear that filtration combustion (FC) can be an effective way to extract energy from biogas with low process costs due to the capacity of burning fuels with low heat content, even those with high impurity concentrations, by skipping the previously-required purification of the gas. Recent applications of FC include volatile organic compound (VOC) emission control, syngas/H2 production from ultra-rich superadiabatic flames, enhancement of internal engine combustion, and thermoelectric generation, among others (Contarin *et al*., 2003a; Contarin *et al*., 2003b; Mujeebu, 2016; Banerjee and Paul, 2021; Hoffman *et al*., 1997).

The technique of reciprocating gas flow direction through the porous medium, also called reciprocal filtration combustion (RFC), can be applied to enhance the efficiency and flammability limits of FC (Ellzey *et al*., 2019). A previous study has investigated RFC of methane in wide ranges of gas flow velocities (0.2 to 0.6 m/s) and equivalence ratio (0.2 to 1.0) (Barcellos *et al*., 2011). This study showed that benefits of RFC included high efficiency, ultra-low emissions, and the expansion of flammability limits. Using this method, in addition to gas flow velocity and equivalence ratio, the half-cycle time (hc) also plays an important role in controlling the energy storage efficiency inside the physical limits of the burner, as denoted by a trapezoidal temperature distribution profile.

Researchers have shown that the peak flame temperature of RFC can be much higher than the adiabatic one (Vandadi *et al*., 2017; Kennedy and Saveliev, 1995). Echigo *et al*. (1995) and *Hanamura et al*. (2005) have suggested the use of RFC for advanced power generation, and its flammability limits have been determined analytically by Hoffmann *et al*. (1996) as well.

Furthermore, periodic reversion of the gas flow direction, in order to confine the combustion zone in a finite length inside the burner, assures transient behavior of filtration combustion. This transience favors the burning of fuel-oxidizer mixtures with ultra-low heat content and remarkably extends its flammability limits. Such is the case of biogas, including situations in which impurity and inert gases are present. (Yao and Saveliev, 2018; Barcellos *et al*., 2011; Barcellos *et al*., 2009). Focusing on NOx emissions in RFC, this technology can achieve values less than 1 up to 15 ppm, burning methane in a wide range of gas velocities (Barcellos *et al*., 2011).

This study is intended to prove that filtration combustion associated with RFC is a viable technical approach to deal with biogas. The experimental investigation will be focused on burning biogas under a wide lean equivalence ratio range (0.1 to 0.9) and gas velocities of 0.2 and 0.3 m/s, expecting to obtain high energy extraction and very low NOx emissions.

EXPERIMENTAL APPARATUS

The experiments on RFC of biogas were performed utilizing methane (the base-fuel) and a synthetic mixture, to simulate a sample obtained from an anaerobic digestion reactor of coconut husk liquor (Leitão *et al*., 2009). Table 1 presents both compositions of biogas collected from the reactor and the synthetic biogas produced in the laboratory, obtained through gas chromatography.

Table 1. Chromatography analysis of biogas samples.

Species	Reactor Sample	Lab Sample
CH_4	74,1%	74,0%
CO_2	21,6%	21,5%
N_2	3,9%	4,2%
ISO-C_4	0,4%	0,3%

The laboratory-scale prototype consists of the following components: (i) the porous burner with heat exchangers embedded at the ends of the porous bed, connected to its water and air-fuel supply systems; (ii) reciprocating electronic-pneumatic system of gas flow; and (iii) the data acquisition system. Fig. 1 illustrates the burner's setup with the main instruments and accessory systems.

Features of the Setup

In this study, a water-tube boiler, developed in antecedent laboratory studies (Barcellos *et al*., 2011) and based on the fundamentals of RFC, was applied. These concepts have been consolidated in a practical mode, encompassing the porous matrix characteristics of the burner, the energy extraction method, the combustion wave control, and the strategies for starting up and maintaining the stability of the combustion process. The porous burner has a cylindrical shape (L_b = 500 mm, D_b = 76.4 mm), in which alumina pellets (D_{pel} = 5.55 mm) create a loose-packed bed, with a porosity of approximately 40%.

The temperature inside the porous medium was measured through S-type thermocouples, linearly arranged at 50, 100, 160, 220, 280, 330, 390, and 450 mm from the bottom flange, and the exhaust temperature was measured by a K-type thermocouple. The water temperature was controlled by resistance temperature detectors (RTD) and its total consumption was measured through a flow transducer and rotameters arranged in each circuit. Air and biogas flows were also measured by rotameters. The NOx emissions were measured with a chemiluminescence analyzer calibrated with 99.995%-N2 and a mixture of

N2+17.6ppm-NO, with the lowest available scale of 0-20ppm. The error ranges of utilized instruments are summarized in Table 2.

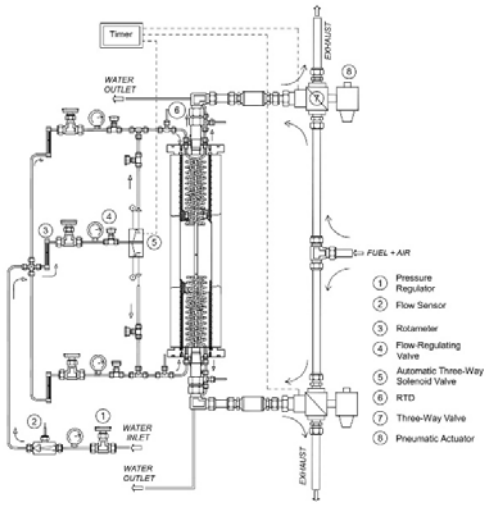

Figure 1. Porous burner equipped with its air and water supply systems and instruments.

Table 2. Measurement error ranges of instruments utilized in the burner.

Instrument	Quantity	Error
Thermocouple "S"	8	0.25% FS
Thermocouple "K"	2	0.75% FS
RTD	6	0.1 °C
Chemiluminescence analyzer	1	4% FS
Rotameter	8	1% FS
Frequency flow transducer	1	1.5% FS

Based on the accuracy of these instruments, the combined uncertainties of temperature, specific power, and energy extraction efficiency were estimated in ±0.8%, ±5.4% and ±10.1%, respectively.

Thermodynamic Parameters

In this study, two main parameters are considered in thermodynamic analysis of filtration combustion: equivalence ratio (Φ) and energy extraction efficiency (η_{ext}). Equivalence ratio is a well-known and essential parameter to results section and represents how close air-fuel mixture is from stoichiometry (Φ = 1), according to Equation 1. For values lower than 1, the mixture is called lean; when higher than 1, rich.

$$\Phi = \frac{\mathrm{Air/Fuel_{real}}}{\mathrm{Air/Fuel_{stoich.}}} \quad (1)$$

Energy extraction efficiency is the fraction of heat, available on fuel, extracted by water that passes through the heat exchangers embedded in reactor's bed. The energy extraction may be calculated by enthalpy raising of water, while the available energy is proportional to the lower heat value of the fuel (LHV), i.e. methane and biogas (Eq. 2). However, as the exchangers are positioned in opposite sides of reactor, heat extraction is much higher is downstream exchanger. Water enthalpies are obtained by temperature and mass flow in both heat exchangers is measured by rotameters (one for upstream and two for downstream, according to Fig. 1).

$$\eta_{ext} = \frac{\left[\dot{m}Cp(\Delta\hat{h})_w\right]_{up} + \left[\dot{m}Cp(\Delta\hat{h})_w\right]_{inf}}{\dot{m}_{fuel}LHV} \quad (2)$$

MATHEMATICAL MODEL

To ensure experimental results were within the range of the operation, a numerical model was utilized to compare the temperature profiles. the model employed is an adaptation of a similar model developed for methane RFC (Contarin et al, 2003b) , in which some input parameters were adjusted appropriately for the incorporation of biogas.

This single-step model can foresee the thermal behavior of the RFC and is capable of predicting the temperature distribution inside the porous medium, considering one dimension only, i.e. the burner's centerline. the solid and gas phases tend to have different temperatures. the gas phase is considered to be a mixture of only two generalized species: the reactants and the products.

Simplifications were employed in order to reduce the degrees of freedom necessary to describe the gas Composition. the chemical reaction is accounted for by a single-step first-order Arrhenius type reaction. The three time-dependent differential equations needed to find the solution are:

Solid phase energy conservation equation (EQ. 3):

$$(1-\epsilon)c_s\rho_s\frac{\partial T_s}{\partial t} = \frac{\partial\left[(k_s^* + k_f)\frac{\partial T_s}{\partial x}\right]}{\partial x} + h_v(T_g - T_s) - \beta(T_s - T_{amb}) \quad (3)$$

Gas phase energy conservation equation (EQ. 4):

$$\epsilon c_g\rho_g\frac{\partial T_g}{\partial t} = \epsilon\frac{\partial\left[(k_g + c_g\rho_g D_{ax})\frac{\partial T_g}{\partial x}\right]}{\partial x} - \epsilon c_g\rho_g v_g\frac{\partial T_g}{\partial x} + h_v(T_s - T_g) + \epsilon H_{chem}W \quad (4)$$

Species conservation equation (EQ. 5):

$$\rho_g\frac{\partial y_p}{\partial t} = \frac{\partial\left[(D + D_{ax})\frac{\partial y_p}{\partial x}\right]}{\partial x} - \rho_g v_g\frac{\partial y_p}{\partial x} + W \quad (5)$$

Where reactant mass consumption rate per unit volume W is given by the Arrhenius law (EQ. 6):

$$W = \rho_g(1 - y_p)A_f\exp\left(\frac{-E_a}{RT}\right) \quad (6)$$

There are only three variables, considering the centerline direction. The boundary conditions applied to the model are presented in Table 3.

It is worth noting that the conditions have been shown in the "x" direction, from x=0 to x=L, so when the flow changes its direction due to the RFC system, the conditions must be adjusted.

Table 3. Boundary conditions applied to the model

Condition	Equation
Gas phase temperature	$T_G(0) = T_0$
Temperature gradient at exit	$\frac{\partial T_G(L)}{\partial X} = 0$
Mass fraction (products) at inlet	$Y_P(0) = 0$
Mass fraction (products) gradient at exit	$\frac{\partial Y_P(L)}{\partial X} = 0$
Thermal conductivity at edges	$K_S(0) = K_S(L) = 0$

Fresh reactants are supplied through the inlet at ambient conditions, and combustion products are exhausted into the atmosphere. After initiation of the combustion wave at one end of the burner, the reaction wave travels back and forth through the bed, defining a temperature profile with a peak temperature near the center of the length of the burner. As time progresses, this profile broadens throughout the length of the burner, presenting a static central temperature plateau inside the burner, ideal for energy extraction or chemical processing.

The numerical predictions were defined utilizing the help of a practical parameter, i.e. a constant heat loss coefficient, β. For both heat exchangers sections, β = 5474 W/(K.m³), while for the central section β = 200 W/(K.m³), representing heat loss through the wall. Since the heat loss coefficient could be computed for each experiment, it was possible to obtain a reasonable estimate of β as function of temperature. This coefficient provides a corrected numerical prediction of experimental efficiencies as a function of the equivalence ratio.

RESULTS AND DISCUSSION

In this study, results refer to the numerical solutions and experiments, with methane (the base-fuel) and biogas samples on the RFC burner prototype. The laboratory experiments encompassed a wide low equivalence ratio range ($0.1 \leq \Phi \leq 0.9$), in which the air-fuel mixture was supplied to the burner at an average temperature of 300 K with gas flow velocities of 0.2 and 0.3 m/s. The following subsections feature results on temperature profiles inside the porous burner, energy extraction, and NOx emissions.

Temperature Profiles

Numerical and experimental results from the RFC burner are presented in Fig. 2. Numerical results from the one-step simulation model also presented reasonable convergence with experimental data, burning methane. Results show the numerical temperature peak values are very close to those obtained from experiments. In addition, the temperature profiles at both the inlet and outlet regions of the porous matrix present numerical and experimental temperature values that are also very similar.

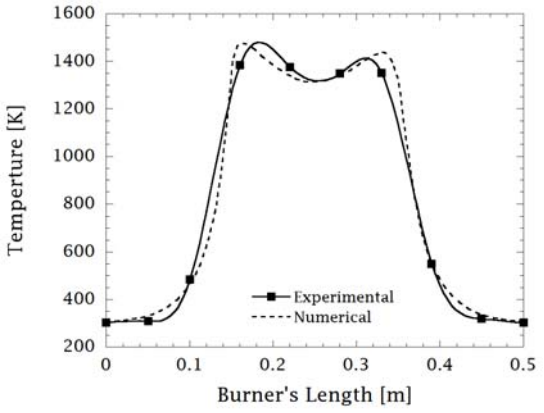

Figure 2. Experimental and numerical temperature distribution profiles from the burner on the RFPB configuration burning methane at Φ=0.5.

By analyzing this figure, it is evident that there are two reaction zones, indicated by the temperature peaks, which are clearly defined in the porous matrix, alternately taking place at specific locations of the burner. As the gas flow is reciprocal, there is a tendency for the flame front to remain at the same positions at each half cycle. It is therefore supposed that the energy storage around the reaction zone makes the medium temperature be more uniform and closer to the reaction zone, favoring when experimental temperature peaks are closer to the numerical ones.

Although the experimental and numerical results present similar values, it is evident that the numerical model achieves a more extended trapezoidal area, pointing out more energy storage inside the porous matrix. Also, it should be noted that the depression on the plateau of the trapezoidal profile correlates with the heat loss at the burner's walls.

Changing the fuel from methane to biogas, features of the temperature profiles practically remain unaltered. Fig. 3 shows both numerical and experimental results from the burner on the RFC, in which the fuel employed in the burner is biogas. For this fuel, the numerical profile is also close to experimental data. However, the experimental temperature profile presents a slight difference to the numerical profile, as its temperature peaks from the simulation are less distant from each other than expected. This difference can be attributed to the effects of CO_2 on the reaction, providing lower

combustion enthalpy and, hence, lower heat stored inside the burner.

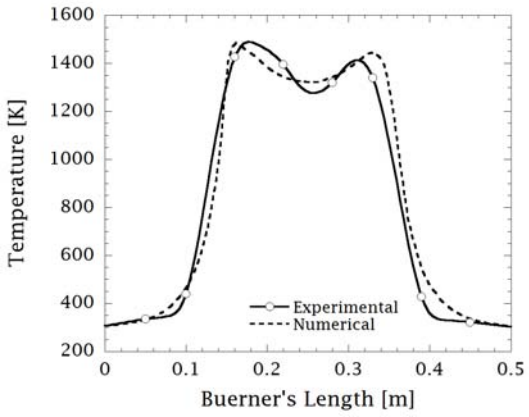

Figure 3. Experimental and numerical temperature distribution profiles from the burner on the RFPB configuration burning biogas at Φ = 0.7.

Fig. 4 shows experimental data from the RFC of biogas at a wide equivalence ratio range. In this case, the temperature profile becomes extended as the equivalence ratio is increased, due to the higher energy storage in the porous matrix, which also slightly increases the temperature peaks and, consequently, more heat to be transferred to the exchangers. For ultra-low equivalence ratios, the temperature profiles correspond to a triangular shape on the middle of the porous matrix independently of the gas flow velocity, as present in Fig. 5. It should be noted that v_g of 0.1 m/s is applied in Fig. 5 to analyze flame front behavior. However, performance parameters are not considered for that v_g because heat exchangers become oversized, drastically reducing efficiency.

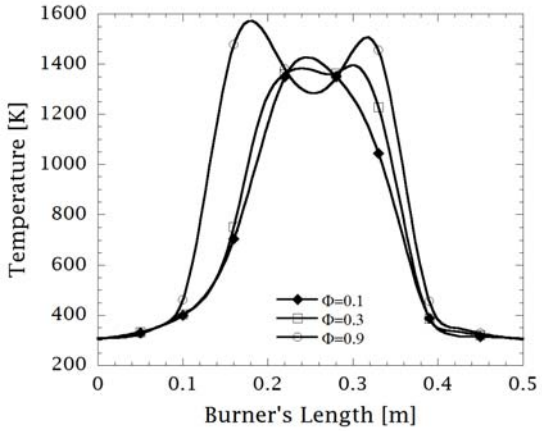

Figure 4. Experimental temperature distribution profiles burning biogas at a wide equivalence ratio range.

Fig. 4 shows that RFC is capable of performing biogas (or methane) burning in a wide equivalence ratio range, including ultra-low values close to 0.1, which would be impossible for conventional burners or in unidirectional FC. The temperature profiles also show that the flame front travels back and forth as a function of the variation of the equivalence ratio and gas flow velocity. Based on experimental results, it should be noted that, in terms of combustion stability, the CO_2 presence in the air-fuel mixture does not significantly affect the burning process of RFC to the point of resulting in flame quenching.

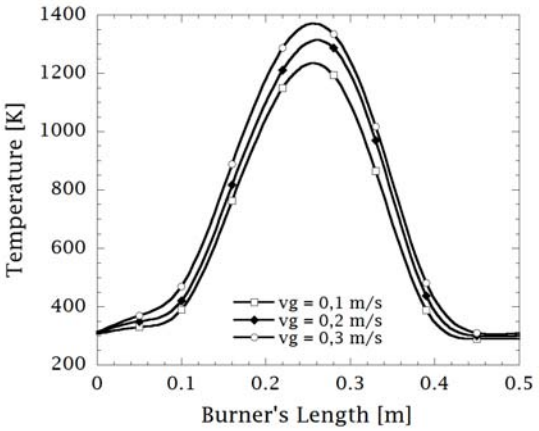

Figure 5. Temperature distribution profile burning biogas at gas flow velocities ranging from 0.1 to 0.3 m/s for a constant ultra-low equivalence ratio of 0.1.

Energy extraction efficiency

Studies of the porous burner prototype, developed based on the filtration combustion concepts, have focused on two goals: ultra-low emissions and high energy extraction efficiency.

As a result, Fig. 6 shows features of the energy extraction process from the porous burner, in which the energy extracted at the equivalence ratio of 0.1 is very low. This is due, in part, to the fact that the burner is relatively long, resulting in a significant portion of heat from the reaction zone being lost through the burner's walls and, consequently, less heat is able to reach the heat exchangers.

Nevertheless, Fig. 7 points out the influence of the gas flow velocity on the extraction efficiency. The efficiency profiles also remain proportionally constant for almost all the equivalence ratio ranges except under ultra-lean operating conditions (Φ < 0.5). The efficiency results were obtained with a laboratory-scale prototype. Therefore, they could be higher as a commercial device considering that, due to the high area-volume ratio, heat loss effects are especially strong in small, experimental setups.

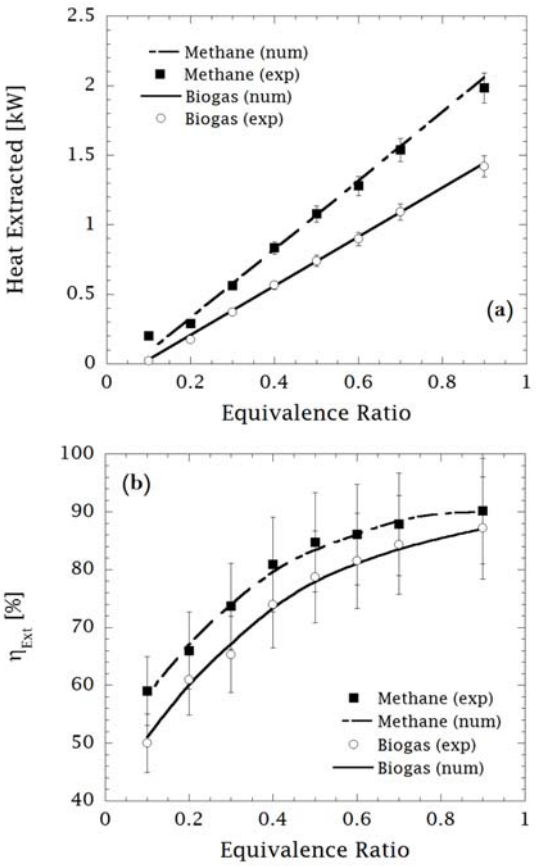

Figure 6. Experimental and numerical results of energy extracted (a) and extraction efficiency (b) at v_g = 0.2 m/s for methane and biogas.

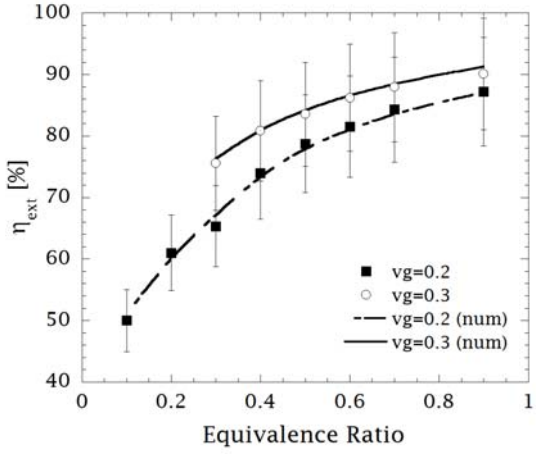

Figure 7. Experimental and numerical results of energy extraction efficiency burning biogas at two different gas flow velocities.

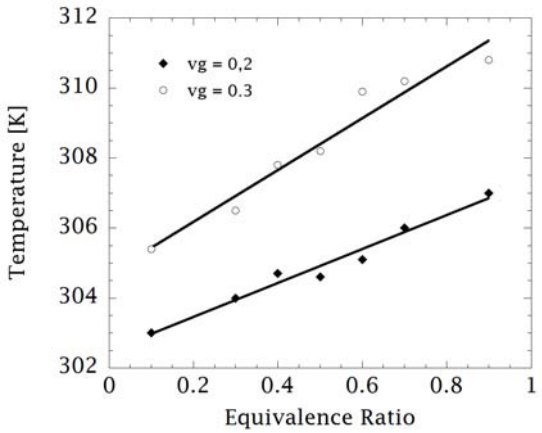

Figure 8. Experimental results of exhaust temperature from the porous burner at different gas flow velocities burning biogas.

Due to high extraction efficiency, the exhaust temperatures are very close to ambient temperature, between 300 and 315 K (Fig. 8). This is likely related to the fact that combustion heat, which would normally be lost by convection through the exhaust is absorbed by the porous medium and transferred to the heat exchangers.

NOx Emissions

In principle, filtration combustion has the unique feature of producing low NOx emissions due to being able to work with ultra-lean air-fuel mixtures, when compared to free flame combustion. It should be noted that under ultra-low equivalence ratio ($\Phi \leq 0.4$) NOx emissions produced by the porous burner are lower than 1.0 ppm. Therefore, some points should be raised in order to explain the NOx formation process, such as:

- The fact that the combustion temperature is low (1300-1600 K), mitigates the NO production through the Zeldovich mechanism; \item It is expected that the N_2O-intermediate mechanism occurs in ultra-lean mixtures.
- Due to the possibility of slightly rich air-fuel mixtures existing in some porous medium interstices, intermediate species such as the radicals OH, CH, HCN, and CN may form, which are important for the Fenimore mechanism.
- Reciprocating filtration combustion leads to a widened homogeneous temperature distribution inside the burner, which favors complete combustion due to the larger residence time for the reactant species.

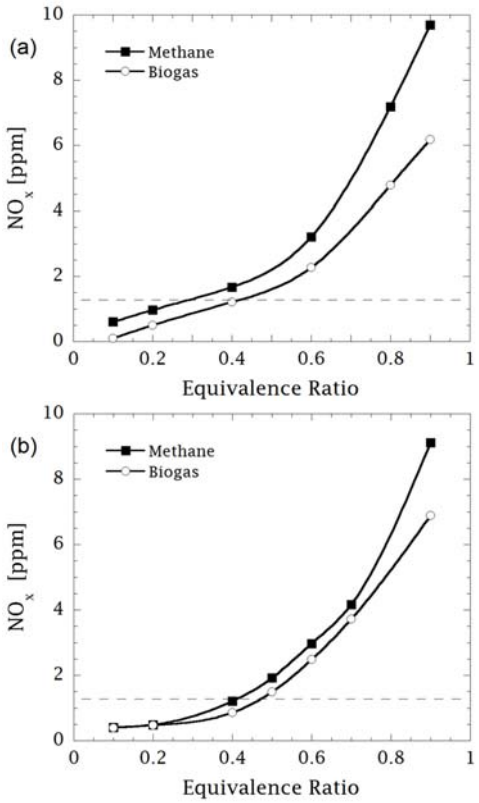

Figure 9. Experimental results about NOx emissions from the porous burner burning methane and biogas: a) v_g = 0.2 m/s and b) v_g = 0.3 m/s. The dashed lines represent the full scale of the analyzer.

Figure 9 shows the influence of the gas flow velocity on the NOx formation. This figure presents experimental results of the two combustible gases, methane and biogas. In both cases, the NOx emissions levels are very low in comparison to values produced by conventional burners. It should be pointed that the graphics show only measures higher than 1 ppm, as that is the minimum value required for accurate results. Measurements taken at lower values are not precise. Although the amount of energy inside the porous medium should be higher as the gas flow velocity is increased, gas flow velocities from 0.2 to 0.3 m/s tends to cool down the reaction zone. As the gas flow velocity continues increasing, energy storage becomes increasingly significant, so that the temperature in the reaction zone reaches higher values and, therefore, NOx emission tends to increase again.

CONCLUSIONS

This study has been important in showing that reciprocal filtration combustion can be successful in the burning of biogas, resulting in the following conclusions:

- With the reciprocating system, the porous burner can extend the flammability limits, either for pure methane or for biogas, toward extremely low equivalence ratio values ($0.1 \leq \Phi \leq 0.9$), maintaining stability and providing ultra-low NOx emissions.
- NOx molar fractions increase from below 1 ppm up to 10 ppm for a wide, ultra-low equivalence ratio range for each fuel used in this study.
- RFC can achieve efficiencies up to 90%, taking into account the wide equivalence ratio range employed in the burner. The numerical results observed using RFC for methane are higher than biogas, as biogas can be burned in RFC as much as methane.
- The system can maintain a high extraction efficiency, up to 85%, with NOx emissions under 2.5 ppm, as obtained in systems with SCR.
- For v_g 0.2 and 0.3 m/s, the system presents low NOx emissions with high efficiency and stability.

REFERENCES

X. Kan, D. Zhou, W. Yang, X. Zhai, C.-H. Wang, An investigation on utilization of biogas and syngas produced from biomass waste in premixed spark ignition engine, Applied Energy 212 (2018) 210 – 222.

A. Matynia, J.-L. Delfau, L. Pillier, C. Vovelle, Comparative study of the influence of CO2 and H2O on the chemical structure of lean and rich methane-air flames at atmospheric pressure, Combustion, Explosion, and Shock Waves 45 (6) (2009) 635.

Y. Kim, N. Kawahara, K. Tsuboi, E. Tomita, Combustion characteristics and NOx emissions of biogas fuels with various CO2 contents in a micro co-generation spark-ignition engine, Applied Energy 182 (2016) 539 – 547.

Z. Wei, H. Zhen, C. Leung, C. Cheung, Z. Huang, Formations and emissions of CO/NO2/NOx in the laminar premixed biogas-hydrogen flame under-going the flame-wall interaction: Effects of the variable CO2 proportion, Fuel 276 (2020) 118096.

L. Xiang, H. Chu, F. Ren, M. Gu, Numerical analysis of the effect of CO2 on combustion characteristics of laminar premixed methane/air flames, Journal of the Energy Institute 92 (5) (2019) 1487–1501.

X. Hu, Q. Yu, Y. Sun, Effects of carbon dioxide on the upper flammability limits of methane in O2/CO2 atmosphere, Energy 208 (2020) 118417.

F. Liu, L. Zheng, R. Zhang, Emissions and thermal efficiency for premixed burners in a condensing gas boiler, Energy 202 (2020) 117449.

A. Maznoy, N. Pichugin, I. Yakovlev, R. Fursenko, D. Petrov, S. S. Shy. Fuel interchangeability for lean premixed combustion in cylindrical radiant burner operated in the internal combustion mode, Applied Thermal Engineering 186 (2021) 115997.

H. Karim, J. Natarajan, V. Narra, J. Cai, S. Rao, J. Kegley, J. Citeno, Staged combustion system for improved emissions operability and flexibility for 7ha class heavy duty gas turbine engine, in: Proceedings of ASME Turbo Expo 2017, no. GT2017-63998, 2017.

J. Hinrichs, M. Hellmuth, F. Meyer, S. Kruse, M. Plümke, H. Pitsch, Investigation of nitric oxide formation in methane, methane/propane, and methane/hydrogen flames under condensing gas boiler conditions, Applications in Energy and Combustion Science 5 (2021) 100014.

X. Cheng, X. T. Bi, A review of recent advances in selective catalytic NOx reduction reactor technologies, Particuology 16 (2014) 1 – 18.

F. Contarin, W. M. Barcellos, A. V. Saveliev, L. A. Kennedy, A porous media reciprocal flow burner with embedded heat exchangers, in: Heat Transfer, Heat Transfer Summer Conference, 2003, pp. 35–42.

F. Contarin, A. V. Saveliev, A. A. Fridman, L. A. Kennedy, A reciprocal flow filtration combustor with embedded heat exchangers: numerical study, International Journal of Heat and Mass Transfer 46 (6) (2003) 949 – 961.

M. A. Mujeebu, Hydrogen and syngas production by superadiabatic combustion – a review, Applied Energy 173 (2016) 210–224.

A. Banerjee, D. Paul, Developments and applications of porous medium combustion: A recent review, Energy 221 (2021) 119868.

J. L. Ellzey, E. L. Belmont, C. H. Smith, Heat recirculating reactors: Fundamental research and applications, Progress in Energy and Combustion Science 72 (2019) 32 – 58.

W. M. Barcellos, L. C. E. Souza, A. V. Saveliev, L. A. Kennedy, Ultra-low emission steam boiler constituted of reciprocal flow porous burner, Experimental Thermal and Fluid Science 35 (3) (2011) 570 – 580.

V. Vandadi, H. Wu, O. C. Kwon, M. Kaviany, C. Park, Multiscale thermal nonequilibria for record superadiabatic-radiant-burner efficiency: Experiment and analyses, International Journal of Heat and Mass Transfer 106 (2017) 731–740.

L. A. Kennedy, A. V. Saveliev, Superadiabatic combustion in porous media: Wave propagation, instabilities, new type of chemical reactor, International Journal of Fluid Mechanics Research (1995) 1–26.

R. Echigo, K. Tawata, H. Yoshida, S. Tada, Effective heating/cooling method for porous thermoelectric device in reciprocating flow combustion system, in: Proceedings of ASME JSME Thermal Engineering Joint Conference, Vol. 4, 1995, pp. 389–396.

K. Hanamura, T. Kumano, Y. Iida, Electric power generation by superadiabatic combustion in thermoelectric porous element, Energy 30 (2) (2005) 347–357, 3rd International Symposium on Advanced Energy Conversion Systems and Related Technologies.

J. G. Hoffman, R. Echigo, S. Tada, H. Yoshida, Analytical study on flammable limits of reciprocating superadiabatic combustion in porous media, Transport Phenomena in Combustion 2 (1996) 1430–1440.

Z. Yao, A. V. Saveliev, High efficiency high temperature heat extraction from porous media reciprocal flow burner: Time-averaged model, Applied Thermal Engineering 143 (2018) 614 – 620.

W. M. Barcellos, L. Souza, I.B.C.Aguiar, A. Saveliev, Hydrogen synthesis in a reciprocal flow porous reactor with energy extraction, in: ECOS 2009415 - 22ND International Conference on Efficiency, Cost, Optimization, Simulation, and Environmental Impact of Energy Systems, ABCM, 2009, pp. 1837–1846.

R. Leitão, A. Araujo, M. Freitas-Neto, M. Rosa, S. Santaella, Anaerobic treatment of coconut husk liquor for biogas production, Water science and technology: a journal of the International Association on Water Pollution Research 59 (2009) 1841–6.